AFRL-SR-AR-TR-09-0054

# REPORT DOCUMENTATION PAGE



**PLEASE DO NOT RETURN YOUR FORM TO THE ABOVE ORGANIZATION.**

| 1. REPORT DATE *(DD-MM-YYYY)* | 2. REPORT TYPE | 3. DATES COVERED *(From - To)* |
|---|---|---|
| 22-02-2009 | Final | 01-03-2005 to 30-11-2008 |

**4. TITLE AND SUBTITLE**
Algorithm Development for the Two-Fluid Plasma Model

**5a. CONTRACT NUMBER**
FA9550-05-1-0159

**5b. GRANT NUMBER**
FA9550-05-1-0159

**5c. PROGRAM ELEMENT NUMBER**

**6. AUTHOR(S)**
Uri Shumlak

**5d. PROJECT NUMBER**

**5e. TASK NUMBER**

**5f. WORK UNIT NUMBER**

**7. PERFORMING ORGANIZATION NAME(S) AND ADDRESS(ES)**
University of Washington
Aerospace & Energetics Research Program
Box 352250
Seattle, WA 98195-2250

**8. PERFORMING ORGANIZATION REPORT NUMBER**

**9. SPONSORING/MONITORING AGENCY NAME(S) AND ADDRESS(ES)**
Dr. Fariba Fahroo
Program Manager, Computational Mathematics
AFOSR/NL
875 N. Randolph St, Rm 3112
Arlington, VA 22203

**10. SPONSOR/MONITOR'S ACRONYM(S)**
AFOSR/NL

**11. SPONSOR/MONITOR'S REPORT NUMBER(S)**

**12. DISTRIBUTION/AVAILABILITY STATEMENT**
Approved for public release

**13. SUPPLEMENTARY NOTES**

**14. ABSTRACT**

A new algorithm is developed based on the two-fluid plasma model that is more physically accurate and capable than MHD models. The algorithm uses high-order spatial and temporal accuracy to simulate time-dependent, three-dimensional plasma phenomena. High-order spatial accuracy is accomplished using a discontinuous Galerkin finite element method that has provided up to 16th order accuracy. The temporal evolution is advanced using a 3rd order Runge-Kutta method. The numerical fluxes are calculated using an approximate Riemann solver based on the two-fluid plasma model. The source terms of the two-fluid plasma model couple the electron and ion fluids to the electromagnetic fields. The simultaneous solution and evolution must be tightly coupled to prevent unstable numerical oscillations. Asymptotic approximations are individually applied to the two-fluid plasma model to approach the Hall-MHD plasma model. An improved method of plasma simulation is found by using the two-fluid plasma model with an artificially increased electron to ion mass ratio and decreased speed of light. Multiscale effects are discovered in current-carrying plasma where small-scale electron instabilities lead to ion shocks that produce large-scale disruptions on the plasma.

**15. SUBJECT TERMS**
high-order algorithms, multiscale physics, mathematically stiff equations

| 16. SECURITY CLASSIFICATION OF: | | | 17. LIMITATION OF ABSTRACT | 18. NUMBER OF PAGES | 19a. NAME OF RESPONSIBLE PERSON |
|---|---|---|---|---|---|
| a. REPORT | b. ABSTRACT | c. THIS PAGE | | | Uri Shumlak |
| U | U | U | UU | 18 | 19b. TELEPHONE NUMBER *(Include area code)* 206-616-1986 |

Final Performance Report (3/1/05 – 11/30/08)

AFOSR Grant No. FA9550-05-1-0159

# "ALGORITHM DEVELOPMENT FOR THE TWO-FLUID PLASMA MODEL"

Submitted to

Dr. Fariba Fahroo
Program Manager, Computational Mathematics
Air Force Office of Scientific Research / NL
875 N. Randolph St, Rm 3112
Arlington, VA 22203

University of Washington
Department of Aeronautics and Astronautics
Aerospace & Energetics Research Program
Box 352250
Seattle, WA 98195-2250

Dr. Uri Shumlak
Principal Investigator

2/17/09

# ALGORITHM DEVELOPMENT FOR THE TWO-FLUID PLASMA MODEL

AFOSR Grant No. FA9550-05-1-0159

U. Shumlak

Department of Aeronautics and Astronautics
Aerospace & Energetics Research Program
University of Washington

**Abstract**

A new algorithm is developed based on the two-fluid plasma model that is more physically accurate and capable than MHD (magnetohydrodynamic) models. The algorithm uses high-order spatial and temporal accuracy to simulate time-dependent, three-dimensional plasma phenomena. High-order spatial accuracy is accomplished using a discontinuous Galerkin finite element method that has provided up to $16^{\text{th}}$ order accuracy. The temporal evolution is advanced using a $3^{\text{rd}}$ order Runge-Kutta method. The numerical fluxes are calculated using an approximate Riemann solver based on the two-fluid plasma model. The source terms of the two-fluid plasma model couple the electron and ion fluids to the electromagnetic fields. The simultaneous solution and evolution must be tightly coupled to prevent unstable numerical oscillations. Electromagnetic fields are solved by both formulating Maxwell's equations as perfectly hyperbolic equations and by using a mixed potential formulation which automatically satisfies the divergence constraint relations. Asymptotic approximations are individually applied to the two-fluid plasma model to approach the Hall-MHD plasma model. An improved method of plasma simulation is found by using the two-fluid plasma model with an artificially increased electron to ion mass ratio and decreased speed of light. Multiscale effects are discovered in current-carrying plasma where small-scale electron instabilities lead to ion shocks that produce large-scale disruptions on the plasma.

# 1 Executive Summary

This project represents a three year effort to develop a new algorithm for plasma simulations based on the two-fluid plasma model. Current plasma simulation algorithms capable of complex geometries are based on the MHD (magnetohydrodynamic) model. The derivation of the MHD model involves several assumptions that severely limit its applicability. The two-fluid model only assumes local thermodynamic equilibrium and is, therefore, more physically

accurate and capable than MHD models. The two-fluid model is formulated in conservation form. An approximate Riemann solver is developed for the two-fluid plasma model to compute the fluxes in a stable and accurate manner. Several methods are investigated to solve the electromagnetic field model, which includes the source terms and divergence constraints. These methods include a characteristic-based algorithm, a perfectly hyperbolic modification, and a mixed potential formulation. The two plasma fluids and the electromagnetic fields communicate through the source terms. The fluid momentum and energy equations have source terms that depend on $\mathbf{E}$ and $\mathbf{B}$. The electromagnetic equations have source terms that depend on $\mathbf{v}_i$ and $\mathbf{v}_e$ (Ampere's law) and $n_i$ and $n_e$ (Gauss's equation). Accurately coupling the source terms is important both for numerical stability and for modeling plasmas where large equilibrium forces exist.

An algorithm is developed for the complete two-fluid plasma model initially in one dimension. The algorithm uses a Roe-type approximate Riemann solver [1] to discretize the hyperbolic fluxes of the fluid model and an upwind characteristic-based solver for the electromagnetic fields. Simulations from the resulting finite volume algorithm are benchmarked against known analytical results. Furthermore, the algorithm is applied to the electromagnetic plasma shock problem to reveal the transition from gas dynamic shock to MHD shock. The results are analyzed to reveal the fast plasma waves that are captured in the two-fluid plasma model. [2]

A high-order algorithm is developed that uses a discontinuous Galerkin, finite element method for the spatial representation and a TVD Runge-Kutta method for the time advance. [3] Solutions are found with up to $16^{\text{th}}$ order spatial accuracy and $3^{\text{rd}}$ order temporal accuracy. The two-fluid plasma algorithm is used to model multiscale physics of current-carrying plasmas, such as the Z-pinch [4] and the field reversed configuration (FRC) [5]. These plasma configurations balance large equilibrium forces between the plasma pressure and the electromagnetic pressure. The high-order algorithm is seen to significantly improve the ability to maintain equilibrium with no artificial decay.

The divergence constraints of Maxwell's equations can be difficult to satisfy with the presence of current and charge sources on an arbitrary computational grid. The divergence constraints are satisfied by reformulating Maxwell's equations to include correction potentials. The approach involves coupling the divergence constraint equations with the time-dependent field equations to form a perfectly hyperbolic equation set. [6] An alternative formulation of Maxwell's equations using mixed potential is also implemented. The mixed potential formulation automatically satisfies the divergence constraints.

This project was performed by Prof. Uri Shumlak and graduate students Ammar Hakim, Robert Lilly, John Loverich, Bhuvana Srinivasan, and Andrec Susanto. This project resulted in doctoral dissertations and master thesis:

- John Loverich, "A Discontinuous Galerkin Method for the Two-Fluid Plasma System and Its Application to the Z-Pinch", Ph.D. 2005.

- Ammar Hakim, "High Resolution Wave Propagation Schemes for Two-Fluid Plasma Simulations", Ph.D. 2006.
- Bhuvana Srinivasan, "A Comparison between the Discontinuous Galerkin Algorithm and the High Resolution Wave Propagation Algorithm for the Full Two-Fluid Plasma Model", M.S. 2005.

These dissertations and theses can be obtained from the University of Washington library system or from the project website, http://www.aa.washington.edu/cfdlab/. Archival journal and conference papers were published reporting on the work from this project:

- J. Loverich and U. Shumlak, "A discontinuous Galerkin method for the full two-fluid plasma model", *Computer Physics Communications* **169** 251-255 (2005).
- A. Hakim, J. Loverich, and U. Shumlak, "High resolution wave propagation scheme for ideal two-fluid plasma equations", *Journal of Computational Physics* **219** (1), 418-442 (2006).
- J. Loverich and U. Shumlak, "Non-linear two-fluid study of $m$=0 sausage instabilities in an axisymmetric Z-pinch", *Physics of Plasmas* **13**, 082310 (2006).
- A. Hakim and U. Shumlak, "Two-fluid physics and field-reversed configurations", *Physics of Plasmas* **14**, 055911 (2007).

# 2 Project Results

Plasmas are essential to many technologies that are important to the Air Force, some of which have dual-use potential. These applications include portable pulsed power systems, high power microwave devices, drag reduction for hypersonic vehicles, advanced plasma thrusters for space propulsion, nuclear weapons effects simulations, radiation production for counter proliferation, and fusion for power generation. In general, plasmas fall into a density regime where they exhibit both collective (fluid) behavior and individual (particle) behavior. The intermediate regime complicates the computational modeling of plasmas.

## 2.1 Plasma Models — Kinetic, PIC, MHD, Two-Fluid

Plasmas may be most accurately modeled using kinetic theory. The plasma is described by distribution functions in physical space, velocity space, and time, $f(\mathbf{x}, \mathbf{v}, t)$. The evolution of the plasma is then modeled by the Boltzmann equation.

$$\frac{\partial f_\alpha}{\partial t} + \mathbf{v}_\alpha \cdot \frac{\partial f_\alpha}{\partial \mathbf{x}} + \frac{q_\alpha}{m_\alpha} (\mathbf{E} + \mathbf{v}_\alpha \times \mathbf{B}) \cdot \frac{\partial f_\alpha}{\partial \mathbf{v}} = \left. \frac{\partial f_\alpha}{\partial t} \right|_{collisions} \tag{1}$$

for each plasma species $\alpha$ = ions, electrons. The Boltzmann equation coupled with Maxwell's equations for electromagnetic fields completely describe the plasma dynamics. [7–9] However, the Boltzmann equation is seven dimensional. As a consequence of the large dimensionality plasma simulations using the Boltzmann equation are only used in very limited applications with narrow distributions, small spatial extent, and short time durations. [10,11] The seven dimensional space is further exacerbated by the high velocity space that is unused except for tail of the distribution or energetic beams. Boundary conditions are difficult to implement in kinetic simulations.

Particle in cell (PIC) plasma model apply the Boltzmann equation to representative superparticles which are far fewer ($10^7$) than the number of particles in the actual plasma ($10^{20}$). [12] PIC simulations have similar limitations as simulations using kinetic theory due to statistical errors caused by the fewer superparticles. Boundary conditions are also difficult to implement in PIC simulations.

The other end of the spectrum in plasma model involves taking moments of the Boltzmann equation and averaging over velocity space for each species which implicitly assumes local thermodynamic equilibrium. The resulting equations comprise the two-fluid plasma model. The two-fluid equations are then combined to form the MHD model. [13] However, in the process several approximations are made which limit the applicability of the MHD model to low frequency and ignores the electron mass and finite Larmor radius effects.

The MHD model treats the plasma like a conducting fluid and assigning macroscopic parameters to describe its particle-like interactions. Plasma simulation algorithms based on the MHD model have been very successful in modeling plasma dynamics and other phenomena. Codes such as MACH2 are based on arbitrary Lagrangian/Eulerian formulations. [14] ALE codes are well suited for simulating plasma phenomena involving moving interfaces. [15] However, ALE codes cannot be formulated as conservation laws and lack many of the inherent conservative properties. The MHD model has been successfully implemented in conservative form to simulate realistic three-dimensional geometries. [16,17]

A severe limitation of the MHD model is the treatment the Hall effect and diamagnetic terms. These terms represent the separate motions of the ions and electrons. The Hall effect and diamagnetic terms also account for ion current and the finite ion Larmor radius. These effects are important in many applications such as electric space propulsion thrusters: Hall thrusters, magnetoplasmadynamic (MPD) thrusters, Lorentz force thrusters. The Hall term is also believed to be important to electrode effects such as anode and cathode fall which greatly affect many directly coupled plasma applications. Furthermore, the Hall and diamagnetic effects may be important for hypersonic flow applications. [18]

The Hall terms can be difficult to stabilize because they lead to the whistler wave branch of the dispersion relation. The phase and group velocities of the whistler wave increase with frequency. The velocities become large even for

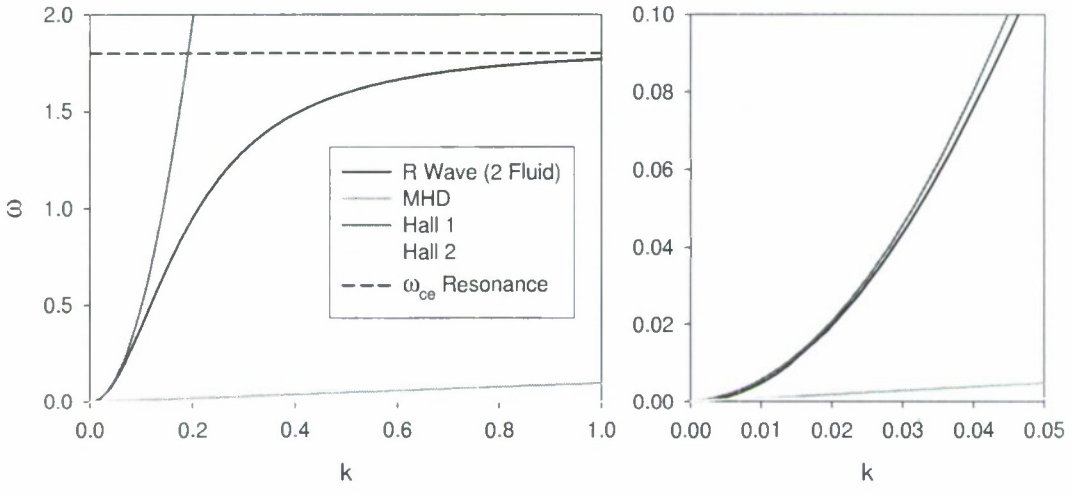


Figure 1: Dispersion relations for the two-fluid plasma model and for the Hall-MHD plasma model that results when asymptotic approximations are applied to the two-fluid plasma model. For small wave numbers and low frequencies (right plot), the upper branch of the Hall-MHD wave follows the R wave of the two-fluid model. However, the waves diverge and the Hall-MHD wave fails to follow the resonance at the cyclotron frequency. The wave speed grows without bound. Artificial hyper-resistivity is required to damp this branch of the Hall-MHD wave.

modest values of the Hall parameter. See Fig. 1 for the dispersion diagram.

A semi-implicit technique has been applied to treat the Hall term in a Hall-MHD model. [19, 20] After the hyperbolic terms of the MHD equations are advanced, the Hall terms are treated independently. The conserved variables are then corrected. The procedure can be computationally intensive. The operator stencil uses 5 points in the sweep direction and 3 points in each orthogonal direction. The complete operator stencil is 45 points. The semi-implicit method works adequately for small Hall parameters, but becomes unstable or slow to converge for the large Hall parameters often seen in applications.

As mentioned above, the two-fluid plasma model is more complete than either the MHD or Hall-MHD model. The two-fluid plasma model resolves plasma oscillations and speed of light propagation. However, many applications are adequately modeled by lower frequency dynamics. Asymptotic approximations ($m_e \to 0$, $c \to \infty$) have been applied to the two-fluid plasma model to eliminate the high frequency waves that limit the maximum numerical time step. Neglecting electron inertia removes the limitation due to the electron plasma and cyclotron frequencies. Infinite light speed removes the limitation due to light transit times. The asymptotic approximations reduce the two-fluid plasma model to the Hall-MHD model. However, applying these approximations fundamentally changes the dispersion relation, as evident in Fig. 1, and

introduces unphysical wave behavior. Specifically, the phase and group velocities of a Hall-MHD wave increase without bound with wave number. The large wave speeds increases the stiffness of the equation system making accurate numerical solutions difficult. Furthermore, the maximum wave number is usually set by either the computational mesh spacing ($k_{max} \propto \Delta x$) or by an artificial resistivity. Rigorous convergence studies are difficult with the simpler plasma models since decreasing $\Delta x$ leads to larger $k_{max}$ and shorter wavelength phenomena.

## 2.2 Two-Fluid Plasma Algorithm

The complexity of the two-fluid model is greater the MHD model but significantly less than the kinetic model. In this project a new algorithm is developed that solves the two-fluid plasma model using an approximate Riemann solver. [2] The method tracks the wave propagation across the domain based on conservation laws.

The two-fluid plasma model captures the separate motion of the electrons and ions without the added complexity of the kinetic model. The two-fluid model is derived by taking moments of the Boltzmann equation for each species. The process of taking moments eliminates the velocity space and yields representative fluid variables (density, momentum, energy) for each species. The only approximation made is local thermodynamic equilibrium within each fluid and is, therefore, a generalization of the MHD model. The fundamental variables are generated by taking moments of the distribution function.

The evolution of the particle density of the ions and electrons is expressed by continuity equations. The equations are the zeroth moment of the Boltzmann equation.

$$\frac{\partial n_i}{\partial t} + \nabla \cdot \left( \frac{\mathbf{j}_i}{q} \right) = 0 \tag{2}$$

$$\frac{\partial n_e}{\partial t} - \nabla \cdot \left( \frac{\mathbf{j}_e}{e} \right) = 0 \tag{3}$$

where $n_i$, $n_e$ are the ion and electron number densities and the particle fluxes are defined by the partial current densities $\mathbf{j}_i = q n_i \mathbf{v}_i$ and $\mathbf{j}_e = -e n_e \mathbf{v}_e$ in terms of the charges $q$, $e$ and fluid velocities $\mathbf{v}_i$, $\mathbf{v}_e$ for the ion and electron fluids.

The first moment of the Boltzmann equation yields momentum equations for each species. The momentum equations are written in divergence form.

$$\frac{\partial \mathbf{j}_i}{\partial t} + \nabla \cdot \left( \frac{\mathbf{j}_i \mathbf{j}_i}{q n_i} + \frac{q}{m_i} p_i \mathbf{I} \right) = \frac{q^2 n_i}{m_i} \mathbf{E} + \frac{q}{m_i} \mathbf{j}_i \times \mathbf{B} + \frac{q}{m_i} \mathbf{R}_{ei} \tag{4}$$

$$\frac{\partial \mathbf{j}_e}{\partial t} - \nabla \cdot \left( \frac{\mathbf{j}_e \mathbf{j}_e}{e n_e} + \frac{e}{m_e} p_e \mathbf{I} \right) = \frac{e^2 n_e}{m_e} \mathbf{E} - \frac{e}{m_e} \mathbf{j}_e \times \mathbf{B} + \frac{e}{m_e} \mathbf{R}_{ei} \tag{5}$$

where $\mathbf{E}$ and $\mathbf{B}$ are the electric and magnetic fields, $p_i$ and $p_e$ are the ion and electron partial pressures, and $\mathbf{R}_{ei}$ is the electron to ion momentum transfer vector.

The second moment of the Boltzmann equation yields energy equations for each species which are expressed in divergence form for the total energy.

$$\frac{\partial \varepsilon_i}{\partial t} + \nabla \cdot \left[ (\varepsilon_i + p_i) \frac{\mathbf{j}_i}{e n_i} \right] = \mathbf{j}_i \cdot \left( \mathbf{E} + \frac{\mathbf{R}_{ei}}{e n_i} \right) \tag{6}$$

$$\frac{\partial \varepsilon_e}{\partial t} - \nabla \cdot \left[ (\varepsilon_e + p_e) \frac{\mathbf{j}_e}{e n_e} \right] = \mathbf{j}_e \cdot \left( \mathbf{E} + \frac{\mathbf{R}_{ei}}{e n_e} \right) \tag{7}$$

where the total energy is defined by

$$\varepsilon_i \equiv \frac{1}{\gamma - 1} p_i + \frac{1}{2} n_i m_i v_i^2 \tag{8}$$

and

$$\varepsilon_e \equiv \frac{1}{\gamma - 1} p_e + \frac{1}{2} n_e m_e v_e^2. \tag{9}$$

where $\gamma$ is the ratio of specific heats and $T_i$, $T_e$ are the ion and electron temperatures. An adiabatic equation of state is assumed. The temperatures are related to the partial pressures by $p_\alpha = n_\alpha T_\alpha$ for $\alpha = \{i, e\}$.

The equations that govern the ion and electron fluids are rewritten in compact, conservative form.

$$\frac{\partial Q}{\partial t} + \nabla \cdot \mathbf{F} = S \tag{10}$$

where $Q$ is the vector of conserved fluid variables, $\mathbf{F}$ is the tensor of hyperbolic fluxes ($F\hat{x} + G\hat{y} + H\hat{z}$), and $S$ is the vector containing the source terms. The vector of conserved variables is

$$Q = \left[ n_i, n_e, j_{i_x}, j_{i_y}, j_{i_z}, j_{e_x}, j_{e_y}, j_{e_z}, \varepsilon_i, \varepsilon_e \right]^T. \tag{11}$$

for the number densities, electrical current densities, and energy densities. The flux Jacobian $\partial F / \partial Q$ for the two fluid equations is constructed in the usual way. The characteristic velocities are calculated to construct the approximate Riemann fluxes.

The eigenvalues of the flux Jacobian give the characteristic velocities.

$$\lambda = \left\{ \frac{j_{i_x}}{e n_i}, \frac{j_{i_x}}{e n_i} \pm \sqrt{\frac{5}{3} \frac{T_i}{m_i}}, -\frac{j_{e_x}}{e n_e}, -\frac{j_{e_x}}{e n_e} \pm \sqrt{\frac{5}{3} \frac{T_e}{m_e}} \right\} \tag{12}$$

The eigenvalues for the two fluid plasma model represent the combination of the drift speeds and thermal speeds for the electrons and ions.

The electromagnetic fields influence the motion of the plasma fluid through the Lorentz force which is contained in Eqs. (4) and (5). The motion of the plasma influences the evolution of the electromagnetic fields through the redistribution of charge density and current density. Maxwell's equation govern the evolution of the electromagnetic fields. The charge density $q n_i - e n_e$ and

current density ($\mathbf{j} = \mathbf{j}_i + \mathbf{j}_e$) are calculated directly from the two-fluid equations which couple the electromagnetic fields.

$$\frac{\partial \mathbf{B}}{\partial t} = -\nabla \times \mathbf{E} \tag{13}$$

$$\epsilon_0 \frac{\partial \mathbf{E}}{\partial t} = \nabla \times \mathbf{B}/\mu_0 - (\mathbf{j}_i + \mathbf{j}_e) \tag{14}$$

$$\epsilon_0 \nabla \cdot \mathbf{E} = q n_i - e n_e \tag{15}$$

$$\nabla \cdot \mathbf{B} = 0 \tag{16}$$

In multiple dimensions the divergence constraints can be difficult to satisfy with the presence of current and charge sources on an arbitrary computational grid. The divergence constraints, Eqs. (15) and (16), are satisfied by reformulating Maxwell's equations to include correction potentials.

The approach involves coupling the divergence constraint equations with the time-dependent field equations to form a perfectly hyperbolic equation set. [6] The field equations are expressed as

$$\frac{\partial \mathbf{B}}{\partial t} + \nabla \times \mathbf{E} + \gamma \nabla \psi = 0, \tag{17}$$

$$\frac{\partial \mathbf{E}}{\partial t} - c^2 \nabla \times \mathbf{B} + \chi c^2 \nabla \phi = -\frac{\mathbf{j}}{\epsilon_0}, \tag{18}$$

$$\frac{1}{\chi} \frac{\partial \phi}{\partial t} + \nabla \cdot \mathbf{E} = \frac{q n_i - e n_e}{\epsilon_0}, \tag{19}$$

$$\frac{1}{\gamma c^2} \frac{\partial \psi}{\partial t} + \nabla \cdot \mathbf{B} = 0, \tag{20}$$

where $\phi$ and $\psi$ are the electric and magnetic correction potentials or, more formally, Lagrange multipliers which vanish at the domain boundaries. The method more accurately predicts the propagation speed of the waves; however, the method can overestimate the Lorentz force caused by charge separation. The implementation illustrates the importance of tightly coupling the field solver to the fluid solver.

The two-fluid plasma model (including the electromagnetic equations) can also be expressed in divergence form.

$$\frac{\partial Q}{\partial t} + \nabla \cdot \mathbf{F} = S \tag{21}$$

where $Q$ is the vector of conserved fluid variables, $\mathbf{F}$ is the tensor of hyperbolic fluxes ($F\hat{x} + G\hat{y} + H\hat{z}$), and $S$ is the vector containing the source terms.

The hyperbolic fluxes are discretized using a Roe-type approximate Riemann solver. [1] In this method the overall solution is built upon the solutions to the Riemann problem defined by the discontinuous jump in the solution

at each cell interface. The numerical flux at the cell interfaces is written in symmetric form as

$$F_{i+1/2} = \frac{1}{2}\left(F_{i+1} + F_i\right) - \frac{1}{2}\sum_k l_k \left(Q_{i+1} - Q_i\right) |\lambda_k| \, r_k \tag{22}$$

where $r_k$ is the $k^{th}$ right eigenvector, $\lambda_k$ is the $k^{th}$ eigenvalue, and $l_k$ is the $k^{th}$ left eigenvector, evaluated at the cell interface $(i + 1/2)$. The values at the cell interface are obtained by a Roe average of the neighboring cells. The flux calculated as above is normal to the cell interface which is the desired orientation for applying the divergence theorem in a finite volume method.

The eigenvalues and eigenvectors of the system flux Jacobians are calculated and properly normalized to prevent catastrophic cancellation. [21, 22] A one-dimensional approximate Riemann solver is developed based on the derived conserved fluxes. [2] Electromagnetic forces are exerted on the plasma fluids through the source terms and the fluid motion affects the fields through the source terms, as shown in Eq. (21). The hyperbolic fluxes are computed accurately by the approximate Riemann solver.

Coupling the source terms to the hyperbolic fluxes is critical for accurate simulations. We have developed a wave propagation algorithm that using a Strang splitting method for the source terms. [23] The hyperbolic fluxes are computed with the approximate Riemann solver. Limiters used on the hyperbolic fluxes and Strang splitting result in a second-order accurate algorithm. However, in equilibrium situations where forces from electromagnetic fields balance fluid pressure or convective forces, the contributions from the source terms must be accurately calculated to balance the divergence of the hyperbolic fluxes. Even small errors lead to a diffusive behavior. The source terms of Eq. (21) are large, in general, which makes the equation stiff.

## 2.3 High-Order Algorithm for Multiscale Physics

An unsplit, finite-element algorithm is developed that can model the entire two-fluid plasma model, including the source terms, with a high spatial accuracy. [3] The algorithm uses a discontinuous Galerkin spatial representation with a TVD Runge-Kutta time advance. [24–26] The discontinuous Galerkin method is a finite element approach that allows for arbitrarily high order basis functions to model the variation of the system variables. Source terms are automatically coupled. The method currently uses up to sixteenth-order accurate spatial representation with a third-order accurate TVD Runge-Kutta time advance method. The algorithm has been implemented for multiple dimensions and on parallel computer architectures.

The conserved variables of the two-fluid plasma model are modeled with a set of basis functions, $\{v_h\}$. The governing equations, expressed as Eq. (21), are multiplied by each basis function and integrated over the mesh cell volume

$\Omega$. An integral equation is generated for each basis function.

$$\int_\Omega v_h \frac{\partial Q}{\partial t} dV + \oint_{\partial\Omega} v_h \mathbf{F} \cdot d\mathbf{S} - \int_\Omega \mathbf{F} \cdot \nabla v_h dV = \int_\Omega v_h S dV \tag{23}$$

where the divergence theorem has been applied to the second term. The volume and surface integrals are replaced with Gaussian quadrature. The flux $\mathbf{F}$ is computed with the approximate Riemann solver with a limiter applied directly to the conserved variables to get high resolution. Less accurate Lax fluxes also typically produce adequate results with reduced computation. The source terms are described by the basis functions and are, therefore, the same order accurate as the solution variables. The high-order representation of the solution variables satisfies the accuracy requirement to preserve the equilibrium balance between the divergence of the hyperbolic fluxes and the source terms. Furthermore, the source terms are directly included in the time advance of the solution variables, and no source splitting is necessary.

The discontinuous Galerkin algorithm has been applied to the electromagnetic plasma shock demonstrating the transition from gas dynamic shocks to the MHD shock [21, 22] as the Larmor radius is reduced. Analysis of the data shows the differences caused by the additional plasma waves that are captured in the two-fluid model and, consequently, in the algorithm developed here. [2] It also illustrates the dispersive nature of the waves which makes capturing the effect difficult in MHD algorithms. The electromagnetic plasma shock serves to validate the algorithm to published data (MHD limit) and analytical results (gas dynamic limit). The algorithm has also been applied to study collisionless reconnection and the results are compared to published results of the GEM challenge (Geospace Environmental Modeling Magnetic Reconnection Challenge) problem. [27] The problem is difficult to model and provides a rigorous test for the algorithm and benchmarks to other algorithms. The evolution of the reconnected magnetic flux compares remarkably well with the published data. [3] Additional applications are discussed in more detail below.

The electromagnetic field model includes divergence constraint relations, which if not accurately satisfied, can lead to nonphysical solutions. Special treatment is required because the divergence relations over-constrain the solution. Satisfying the divergence constraint relations can be accomplished using a Hodge projection, which requires solving elliptic equations over the entire spatial domain, or by adding correction potentials to form perfectly hyperbolic equations, which requires solving additional hyperbolic equations to sweep the divergence error out of the domain, as described above. Alternative to these approaches, Maxwells equations can be formulated using scalar and vector potentials that automatically satisfy the divergence constraint relations. The mixed potential formulation is expressed as

$$\frac{\partial^2 \phi}{\partial t^2} - \nabla^2 \phi = q n_i - e n_e, \frac{\partial^2 \mathbf{A}}{\partial t^2} - \nabla^2 \mathbf{A} = \mathbf{j}_i + \mathbf{j}_e, \tag{24}$$

assuming a Lorentz gauge condition. The mixed potential formulation is implemented by solving the hyperbolic equations, given by Eq. (24), as a set of

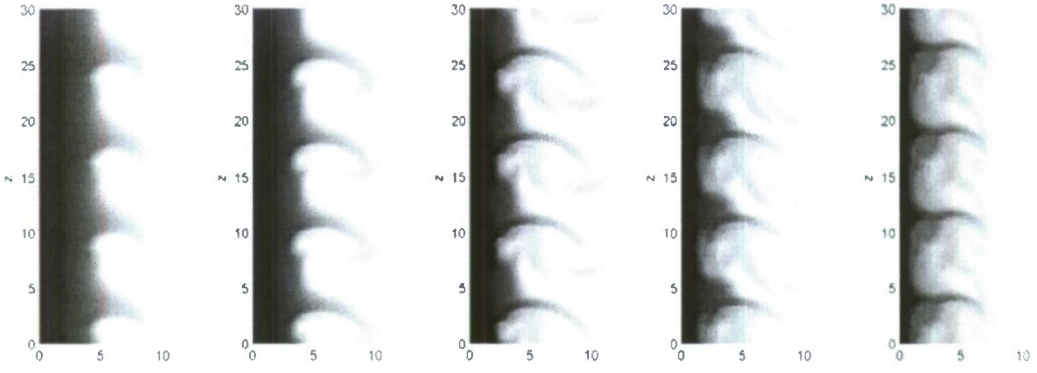


Figure 2: Evolution of an axisymmetric, two-fluid Z-pinch with an initial small, sinusoidal perturbation with four periods showing the ion density contours. Only the final stages of the evolution are shown; $t = 25$, 30, 35, 40, and 45. The perturbation remains small until late in time when the mode becomes unstable. The bending of the mode is an expected two-fluid result caused by the finite electron mass. Spatial scales are expressed in ion Larmor radii. $r_{Li}/a = 7.5$.

first-order hyperbolic equations by defining auxiliary variables. The gauge condition then becomes an algebraic expression in terms of the auxiliary variables. A related approach is to assume electromagnetic waves propagate instantaneously, $c \to \infty$, known as the Darwin approximation. [28] This approach has been implemented as part of the asymptotic approximations described above.

## 2.4 Applications

### 2.4.1 Multiscale Structures in a Z-pinch

The algorithm has been applied to study hybrid plasma instabilities in Z-pinch geometries. [4] The results are applicable to Z-pinches experimentally studied at UW and Sandia National Labs. An axisymmetric, two-fluid Z-pinch equilibrium is initialized with periodic boundaries in the axial direction. A 1%, sinusoidal perturbation of the azimuthal magnetic field is applied and the plasmas dynamical response is followed. The effect of two-fluid physics can be seen by adjusting the normalized ion Larmor radius, $r_{Li}/a$, where $a$ is the pinch radius. Figure 2 shows the evolution of the ion density for during the final stages of an instability; $t = 25$, 30, 35, 40, and 45. A four period perturbation is applied. The applied mode is seen to grow eventually entering into the nonlinear regime and finally plasma confinement is destroyed. The protruding plasma bends downward due to an expected two-fluid phenomena — the finite electron inertia influences the ion density.

When the plasma size is reduced, $r_{Li}/a = 2.5$, the plasma evolution changes dramatically as seen in Fig. 3. The ion density contours are shown at $t = 10$

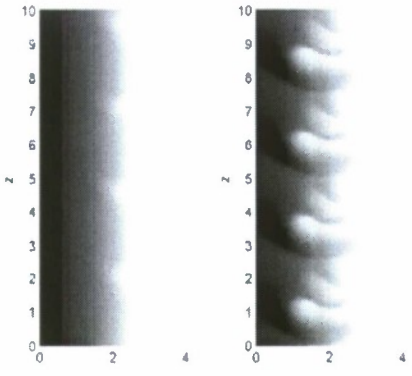


Figure 3: Evolution of an axisymmetric, two-fluid Z-pinch with an initial small, sinusoidal perturbation with four periods showing the ion density contours. The earlier stages of the evolution are shown; $t = 10$ and 15. The plasma has $r_{Li}/a = 2.5$. The perturbation at $t = 10$ looks similar to Fig. 2. However, at $t = 15$ the four-period perturbation is overtaken by a shorter wavelength mode.

and 15. The same equilibrium and perturbation have been applied, and the four-period perturbation is evident at $t = 10$. As the plasma evolves a shorter wavelength mode grows and quickly overtakes the initialized perturbation. The mode is independent of the initial perturbation. The wavelength is set by the Larmor radius. The simulation in Fig. 3 has $r_{Li}/L = 10$, so a ten-period mode develops. Furthermore, the finite electron inertia leads to the formation of shocks.

Analyzing the results reveals the instability occurs when the electron drift speed exceeds the ion sound speed. The instability is related to the lower hybrid drift instability. [29] If the electron drift speed is kept below the ion sound speed, results similar to Fig. 2 occur if the equilibrium is MHD unstable. However, if the electron drift speed exceeds the ion sound speed, a mode similar to Fig. 3 occurs. This effect is not seen in MHD plasma models.

### 2.4.2 Lower Hybrid Drift Instability in a Planar Plasma

The algorithm has been applied to study hybrid plasma instabilities in field reversed configuration (FRC) geometries. [5] FRCs are experimentally studied at AFRL and UW. The same effect is observed in planar current-carrying plasma sheets, which are neutrally stable in the MHD model. The simpler geometry and stability properties better isolate the physical mechanism and allow a more thorough investigation. An axisymmetric, two-fluid equilibrium is initialized with periodic boundaries in the longitudinal direction. A single-period, sinusoidal perturbation of the density is applied and the plasmas dynamical response is followed. Results are shown in Fig. 4. The spatial scales are normalized by the ion Larmor radius. The initial perturbation does not grow.

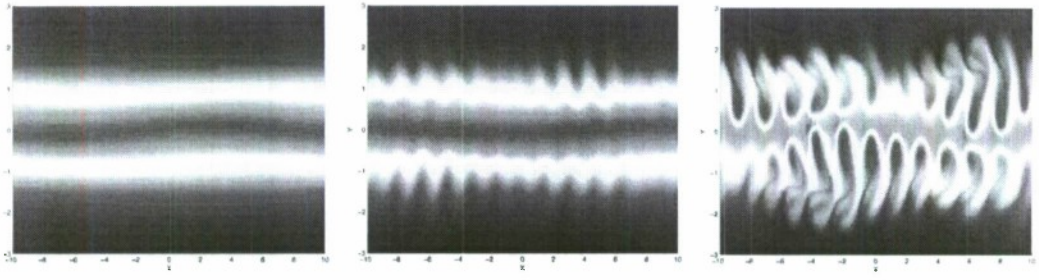

Figure 4: Electron density evolution of a current sheet at $t = 100, 200, 250$. Current is in-plane to the left with a confining magnetic field out-of-plane above and below the current sheet. The initial equilibrium is MHD stable, but develops a lower hybrid drift instability captured by two-fluid effects. By $t = 200$, perturbations with a scale length of the ion Larmor radius are visible. The instability is fully developed by $t = 250$.

Instead, a perturbation with a scale length of the ion Larmor radius develops. The ions separate slightly from the electrons creating an electric field that impedes the current. The finite electron inertia leads to the formation of shocks that give the mode a "fishbone" character.

As in the case of the Z-pinch, the instability occurs when the electron drift speed exceeds the ion sound speed, and if the electron drift speed is kept below the ion sound speed, instabilities do not develop. When the electron drift speed exceeds the ion sound speed, the mode shown in Fig. 4 develops even though the equilibrium is MHD stable.

The instability simulated and identified has practical implications. The lower hybrid drift instability has been suspected as the cause of the "anomalous resistivity" in FRC experiments, particularly those using rotating magnetic field current drive. [30] Numerically computed effective impedance. shows an "anomalous resistivity" that agrees with the experimental observations and leads to cross-field transport.

### 2.4.3 3D Instabilities in a Z-Pinch

Gross three-dimensional instabilities in a Z-pinch have been studied. The Z-pinch results are shown in Fig. 5. The Z-pinch equilibrium is expected to be unstable to gross MHD modes, such as the sausage mode (center plot) and kink mode (right plot). However, an additional, small-scale instability develops on top of the MHD modes. The instability is related to the lower hybrid drift instability. The small-scale structure shown in Fig. 5. is not captured in the Hall-MHD and MHD plasma models.

Figure 5: Electron density evolution of a Z-pinch showing the development of a lower hybrid drift instability superimposed on the sausage and kink MHD modes.

## 2.5 Conclusions

A motivation for implementing the high-order discontinuous Galerkin method is to accurately capture the detailed spatial structure of plasma dynamics without necessitating large computational grids. We have investigated this ability by comparing solutions from the discontinuous Galerkin method with a second-order wave propagation method applied to a variety of hyperbolic problems — linear advection, electrostatic ion cyclotron waves, electromagnetic waves, and two-fluid plasma dynamics. The general finding indicates that for applications with a single characteristic speed or speeds with a limited range, the low-order method adequately captures the solution with substantially less computational effort. However, for applications with disparate characteristic speeds, the high-order method is better able to capture the solution without the phase errors that appear in the low-order method.

The two-fluid plasma model resolves plasma oscillations and speed of light propagation. However, many applications are adequately modeled by lower frequency dynamics. Asymptotic approximations ($m_e \to 0$, $c \to \infty$) have been applied to the two-fluid plasma model to eliminate the high frequency waves that limit the maximum numerical time step. Applying these approximations fundamentally changes the dispersion relation and introduces unphysical wave behavior. Accurate simulations require large computational efforts.

More accurate and less computationally intensive simulations are possible using the two-fluid plasma model with reduced mass ratio and light speed. The high frequency dynamics captured by the two-fluid plasma model is modified by allowing the electron mass to increase, such that the mass ratio $m_i/m_e$ is smaller than the physical value (1836 for hydrogen plasma). We have produced accurate simulations with mass ratios as small as 25. Increasing the mass ratio to 100 does not significantly alter the results. Similarly, the speed of light only needs to be much larger than the next fastest characteristic, typically the

Alfvén speed. The ratio $c/v_A$ is approximately 1000 in experimental plasmas. However, we have produced accurate simulations with values as small as 10. These reduced values provide significant computational speed increases without a significant loss of accuracy.

# Acknowledgment/Disclaimer

This work was sponsored by the Air Force Office of Scientific Research, USAF, under grant number FA9550-05-1-0159. The views and conclusions contained herein are those of the author and should not be interpreted as necessarily representing the official policies or endorsements, either expressed or implied, of the Air Force Office of Scientific Research or the U. S. Government.

# References

[1] P. L. Roe. *Journal of Computational Physics*, 43:357, 1981.

[2] U. Shumlak and J. Loverich. Approximate Riemann solver for the two-fluid plasma model. *Journal of Computational Physics*, 187:620–638, 2003.

[3] J. Loverich and U. Shumlak. A discontinuous Galerkin method for the full two-fluid plasma model. *Computer Physics Communications*, 169:251–255, 2005.

[4] J. Loverich and U. Shumlak. Nonlinear full two-fluid study of m=0 sausage instabilities in an axisymmetric Z pinch. *Physics of Plasmas*, 13:062505, 2006.

[5] A. Hakim and U. Shumlak. Two-fluid physics and field-reversed configurations. *Physics of Plasmas*, 14:055911, 2007.

[6] C. D. Munz, P. Ommes, and R. Schneider. A three-dimensional finite volume solver for the Maxwell equations with divergence cleaning on unstructured meshes. *Computer Physics Communications*, 130:83–117, 2000.

[7] A. R. Bell. Computational Simulation of Plasmas. *Astrophysics and Space Science*, 256:13–35, 1998.

[8] C. Z. Cheng and G. Knorr. *Journal of Computational Physics*, 22:330, 1976.

[9] H. Ruhl and P. Mulser. *Physics Letters A*, 205:388, 1995.

[10] L. Chacón, D. C. Barnes, D. A. Knoll, and G. H. Miley. *Journal of Computational Physics*, 157:618, 2000.

[11] L. Chacón, D. C. Barnes, D. A. Knoll, and G. H. Miley. *Journal of Computational Physics*, 157:654, 2000.

[12] C. K. Birdsall and A. B. Langdon. *Plasma Physics via Computer Simulation*. McGraw-Hill, New York, 1985.

[13] J. P. Freidberg. Ideal magnetohydrodynamic theory of magnetic fusion systems. *Reviews of Modern Physics*, 54(3):801–902, July 1982.

[14] R. E. Peterkin Jr., M. H. Frese, and C. R. Sovinec. Transport of Magnetic Flux in an Arbitrary Coordinate ALE Code. *Journal of Computational Physics*, 140(1):148–171, February 1998.

[15] U. Shumlak, T. W. Hussey, and R. E. Peterkin Jr. Three-Dimensional Magnetic Field Enhancement in a Liner Implosion System. *IEEE Transactions on Plasma Science*, 23(1):83–88, February 1995.

[16] O. S. Jones, U. Shumlak, and D. S. Eberhardt. *Journal of Computational Physics*, 130:231, 1997.

[17] B. Udrea and U. Shumlak. Nonlinear study of spheromak tilt instability. In *AIAA 36th Aerospace Sciences Meeting & Exhibit*, Reno, Nevada, January 1998. AIAA Paper No. 98-0995.

[18] R. E. Peterkin and P. J. Turchi. Magnetohydrodynamic theory for hypersonic plasma flow - what's important and what's not. In *AIAA 31st Plasmadynamics and Lasers Conference*, Denver, Colorado, June 2000. AIAA Paper No. 2000-2257.

[19] D. Harned and Z. Mikic. *Journal of Computational Physics*, 83:1, 1989.

[20] J. T. Becerra Sagredo. Semi-implicit treatment of the hall term in finite volume, mhd computations. Master's thesis, University of Washington, Seattle, WA 98195, June 1998.

[21] M. Brio and C. C. Wu. *Journal of Computational Physics*, 75:400, 1988.

[22] A. L. Zachery and P. Colella. *Journal of Computational Physics*, 99:341, 1992.

[23] A. Hakim, J. Loverich, and U. Shumlak. A high resolution wave propagation scheme for ideal Two-Fluid plasma equations. *Journal of Computational Physics*, 219:418–442, 2006.

[24] B. Cockburn and C.-W. Shu. *Mathematics of Computation*, 52:411, 1989.

[25] B. Cockburn, S. Hou, and C.-W. Shu. *Mathematics of Computation*, 54:545, 1990.

[26] B. Cockburn and C.-W. Shu. *Journal of Computational Physics*, 141:199, 1998.

[27] J. Birn, J. F. Drake, M. A. Shay, B. N. Rogers, R. E. Denton, M. Hesse, M. Kuznetsova, Z. W. Ma, A. Bhattacharjee, A. Otto, and P. L. Pritchett. Geospace Environmental Modeling (GEM) Magnetic Reconnection Challenge. *Journal of Geophysical Research*, 106(2):3715, 2001.

[28] A. N. Kaufman and P. S. Rostler. The Darwin Model as a Tool for Electromagnetic Plasma Simulation. *Physics of Fluids*, 14:446, 1971.

[29] N. A. Krall and P. C. Liewer. Low-Frequency Instabilities in Magnetic Pulses. *Physical Review A*, 4:2094–2103, 1971.

[30] A.L. Hoffman, H.Y. Guo, K.E. Miller, and R.D. Milroy. Principal physics of rotating magnetic-field current drive of field reversed configurations. *Physics of Plasmas*, 13:012507, 2006.